INSTYTUT FIZYKI JĄDROWEJ
Im. Henryka Niewodniczańskiego
Polskiej Akademii Nauk

Ul. Radzikowskiego 152, 31-342 Kraków

WWW.ifj.edu.pl/reports/2012.html

Kraków, grudzień 2012

Report No.2057/AP

OPERATION REGIME OF AIC-144 CYCLOTRON FOR DELIVERING 60 MeV PROTON BEAM TO THE RADIOTHERAPY OF EYE MELANOMA

R. Cieślik, K. Daniel, R. Grzybek, K. Gugula, G. Janik, A. Koczot,
B. Lipka, J. Molęda, T. Norys, W. Pyzioł, M . Ruszel, B. Sałach,
J. Sulikowski, A. Sroka, R. Tarczoń, INP PAS, Krakow, Poland
I. Amirkhanov, G. Karamysheva, I. Kiyan, N. Morozov,
E. Samsonov, JINR, Dubna, Russia

Abstract

The latest computational and experimental results concerning 60 MeV proton beam acceleration and extraction in AIC-144 cyclotron of the Institute of Nuclear Physics (Krakow, Poland) are being considered. Improvement of RF system reliability at dee voltage of 60 kV and frequency of 26.26 MHz as well as precise shaping of the cyclotron magnetic field made it possible to accelerate the proton beam up to 60.5 MeV and to provide its extraction with overall efficiency ~35%. The beam is planned to be used for the long-term radiotherapy of eye melanoma in the year 2013.

Introduction

AIC-144 cyclotron is used in the Institute of Nuclear Physics Polish Academy of Sciences mainly as a source of deuteron and proton beams for isotope production on internal target. During recent years several systems of the cyclotron have been modified in order to provide required parameters of external proton beam with energy of 60 MeV necessary to conduct radiotherapy of eye melanoma which is executed in the Institute since 2011 [1].

Some important efforts have been done to increase the reliability of RF system operation at frequency of 26.26 MHz and dee voltage of 60 kV. Stable work of RF system in this regime provided essential increase in the extraction efficiency of 60 MeV protons.

Magnetic field measurements were fulfilled in order to shape specified level of the isochronous field with required accuracy and to limit the 1-st harmonic of the field imperfections by a value of ~ 5 Gs [2,3].

Particle dynamics computations show that the beam is accelerated up to extraction system with accepted phase drift and amplitudes of transverse oscillations. Main losses of the protons (~40%) occur at radius ~61 cm (energy ~59.5 MeV) due to action of the coupling resonance $Q_r-2Q_z = 0$ and parametric one $2Q_z = 1$.

Experimental study of the beam acceleration and extraction confirms main results of the computations. RF phase of the beam just before the extraction is close to 10°RF as it was measured with Smith and Garren method [4, 5].

Experimental extraction efficiency is ~50% after two electrostatic deflectors in comparison to internal circulating beam intensity and approaches ~35% at a point out of the cyclotron.

1. Improvement of RF system operation

Between 2005 and 2007 the high-frequency system was revamped. The modernization included reducing the contact resistance at the power stage of the generator, the acceleration chamber, the resonator and the chamber connecting the resonator with the acceleration chamber [6].

During the ten-year exploitation some high-frequency elements became stale. In particular, the metal and plating elements (that were grounding and shielding surfaces) got degraded. These elements, in the form of sheets, were connected by bolts and the contact impedance between them was not sufficiently low. As time passed, this impedance, both active and passive, increased due to progressive metal corrosion, loosening of bolts and elements deformation. Particularly disadvantageous was the change of the generator impedance. It resulted in unstable power output and accelerating voltage in the cyclotron.

In order to improve the conductivity and prevent future degradation, copper elements were covered with copper sheets. Welded joints were used in the place of the screwed ones. The contact force was increased and the contacts in the areas where welding was not possible were cleaned (Fig. 1.1).

Reducing the contact resistance for high-frequency current resulted in 50% decrease of power loss and increase in the amplitude of high-frequency voltage on the accelerating electrode from about 50 kV to 60 kV. Attempts to work carried out in autumn 2007 showed in addition improved stability of power output and voltage at the dee edge.

Figure 1.1 Contacts in the high-frequency components of the system.
a. Fragment of the interior of a high-frequency resonator with visible contacts.
b. Welded joint of high-frequency resonator.

2. Last shaping of magnetic field

The last AIC-144 cyclotron magnetic field mapping and shaping campaign was executed in years 2011-2012 [3]. The main goals of this campaign were the following:

- verification of the cyclotron magnetic field in comparison with 2006 mapping one;
- shaping of the new magnetic field regime taking into account new requirements to the central magnetic field bump and increasing the final energy of the accelerated proton beam;
- correction of the 1-st harmonic of magnetic field in the extraction region of cyclotron.

2.1 Verification of the magnetic field

A small (~5 Gs) average magnetic field change in relation to the previous (2006) one at the same conditions of the magnet was observed. This difference was corrected by a small excitation current change ~(5-10) A in the cyclotron trim coils. Fig. 2.1 shows the initial deviation of average magnetic field from the required one and the deviation after the trim coils current correction.

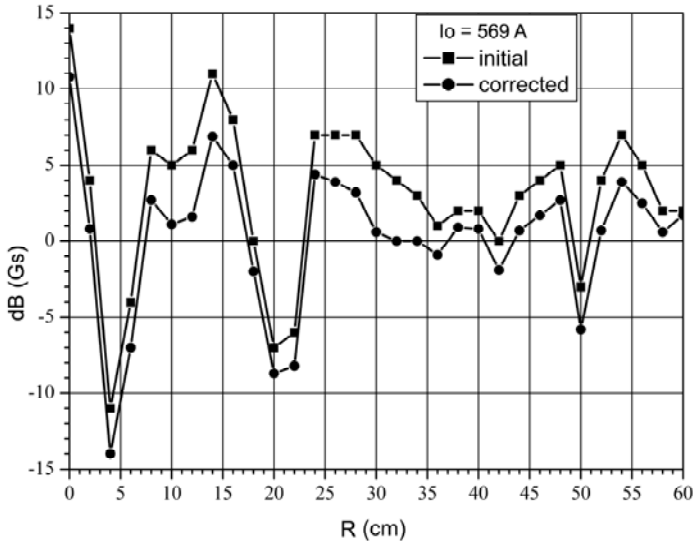

Fig. 2.1. Deviation of the average magnetic field from the required one, main coil current Io = 569 A

2.2 Shaping of the new cyclotron regime

The new cyclotron regime was simulated with the aim of increasing the energy of protons extracted from the cyclotron to supply the eye therapy room with increased penetration possibility. The increasing of final proton energy is demonstrated in Figs. 2.2 and 2.3 versus associated RF frequency and the main coil excitation current, accordingly. The initial regime is assumed as Io=569A, f=26.103 MHz. The new regimes were measured and shaped for the main coil current Io=577, 585, 593, 601, 609, 617, 625, 633, 641 and 649 A. Average magnetic field for some of them is shown in Fig. 2.4.

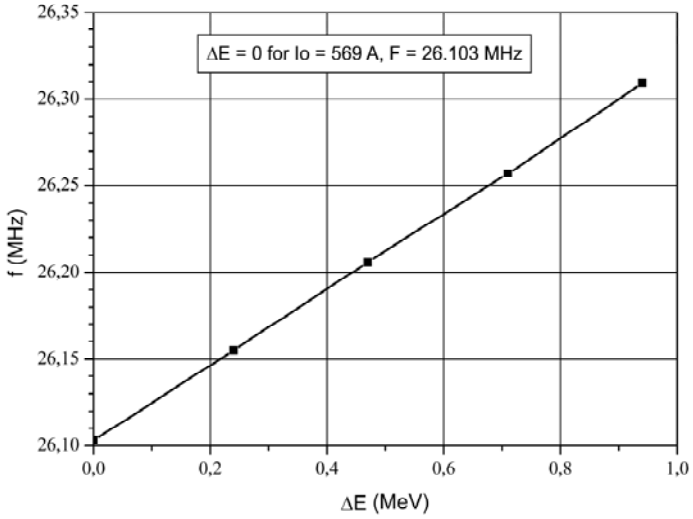

Fig. 2.2. RF frequency versus final proton beam energy change

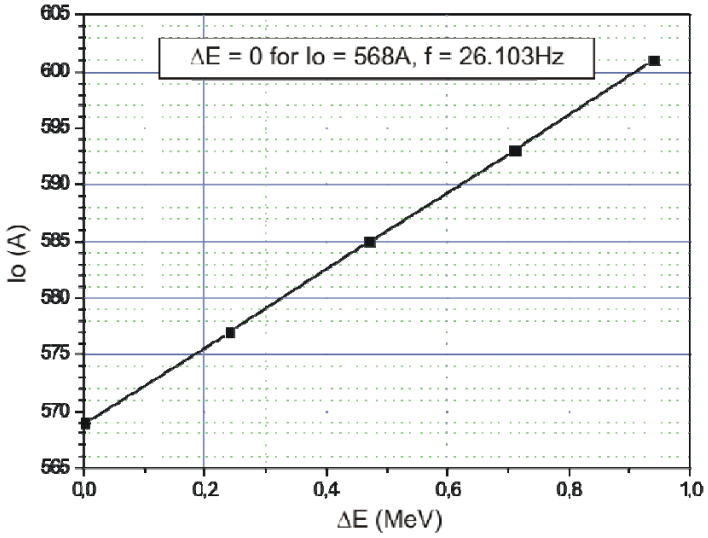

Fig. 2.3. Main coil current versus final proton beam energy change

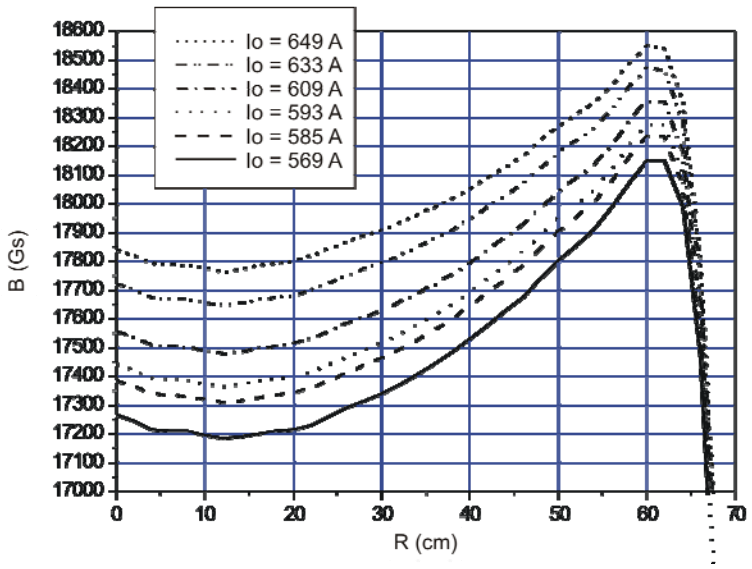

Fig. 2.4. Average magnetic field of cyclotron for different main coil currents

The regime f = 26.26 MHz, Io = 591.5 A was simulated on the basis of a new technique [4] with the help of Cyclotron Operator HELP Program Complex 2004-2012 using main magnetic field maps measured for Io = 570, 585 and 600 A. This regime was simulated with central magnetic field bump ~360 Gs relatively isochronous field and with 230 Gs one (Fig. 2.5). The last bump was experimentally found the most optimal one for the extraction efficiency.

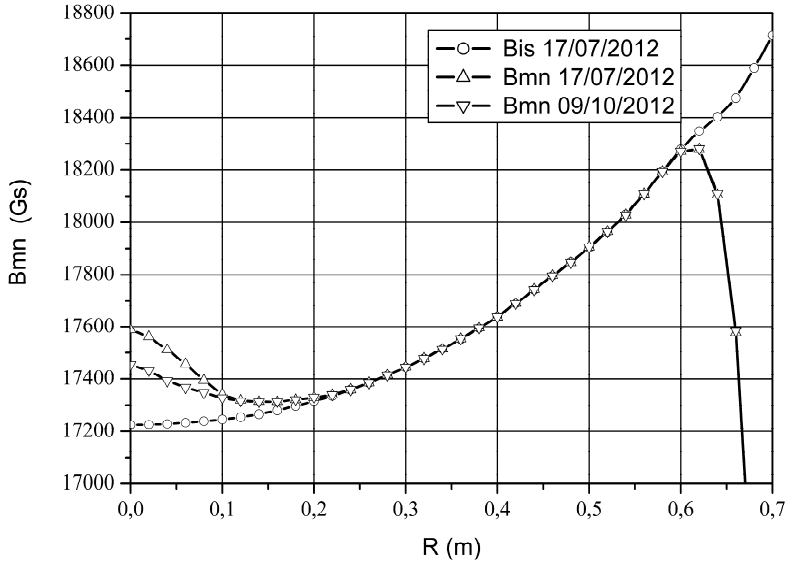

Fig. 2.5. Average magnetic field for regime f = 26.26 MHz, Io = 591.5 A with increased bump (Bmn 17/07/2012) and optimal one (Bmn 09/10/2012)

2.3 Correction of the 1-st harmonic of magnetic field

The extraction efficiency of 60 MeV proton beam after the 2006 magnetic field mapping campaign was mostly at the level ~10%. As the time went by the constant decreasing of the efficiency occurred and at the beginning of 2011 it was at the level of 3%. One of the reasons of such situation is the increase of the 1st harmonic amplitude in the extraction region due to unpredictable horizontal shift of the cyclotron vacuum chamber with iron pole sectors. Before the 2011 magnetic field mapping the cyclotron was equipped with the dedicated mechanical system of the vacuum chamber positioning (Fig. 2.6).

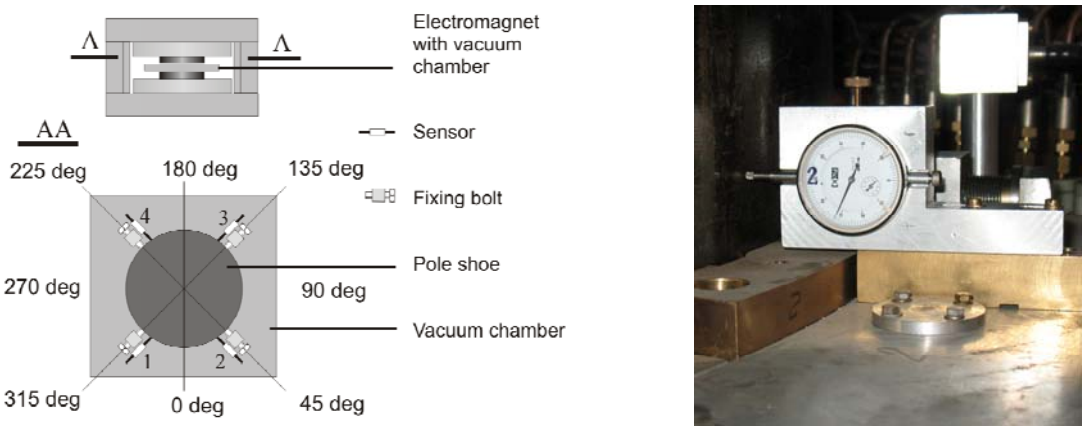

Fig. 2.6. System of vacuum chamber positioning and measurement of its shift

The initial value of the magnetic field 1st harmonic was measured in 2011 at the level ~12-13 Gs at R = 62 cm (Fig 2.7). By the 3 iterations of vacuum chamber horizontal shift the 1st harmonic was decreased to the level about 2 Gs. The vacuum chamber was shifted on 0.46 mm. The characteristics of the 1st harmonic phase before and after vacuum chamber correction are shown in Figs. 2.7 and 2.8. The computations show that these parameters of the 1st harmonic are very good for the beam extraction with high efficiency. However, magnetic channels MC-1 and MC-2 that were not installed in their working position during the field measurements lead to essential change of the 1st harmonic in the extraction region and deteriorating extraction efficiency. Harmonic coils were used to compensate influence of the magnetic channels. Response of the channels and harmonic coils on amplitude of the 1st harmonic was measured a few years ago. Figure 2.9 shows the amplitude of the 1st harmonic with magnetic channels impact and with compensation of this impact by the harmonic coils. Currents in the coils I1 - I3 = 82 A, I2 - I4 = 257 A were found experimentally by obtaining maximum of the extraction efficiency. The resulting amplitude of the 1st harmonic presented in Fig. 2.9 has been applied in simulation of the beam dynamics (see below).

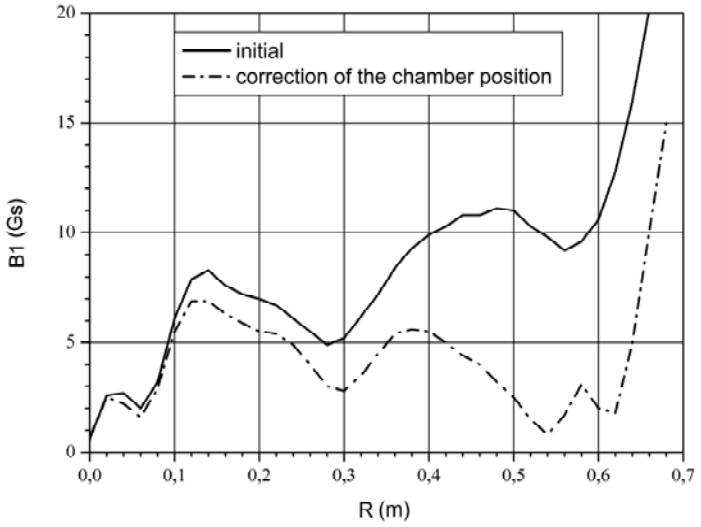

Fig. 2.7. Correction of the magnetic field 1st harmonic by chamber shift

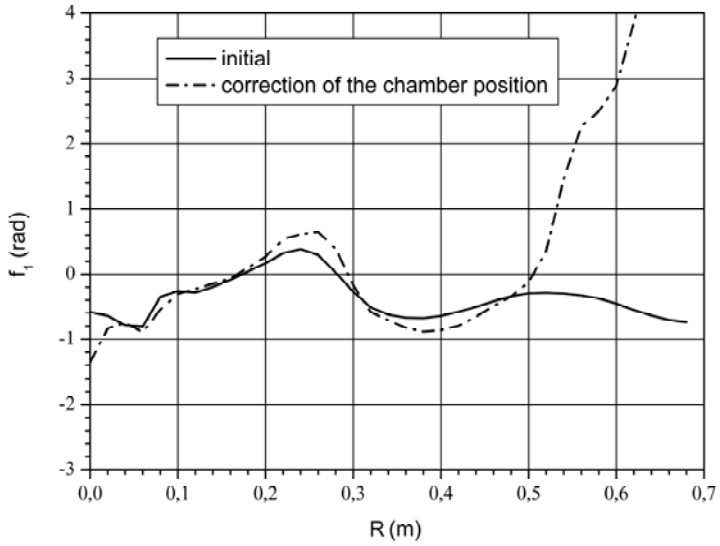

Fig. 2.8. Phase of the magnetic field 1st harmonic

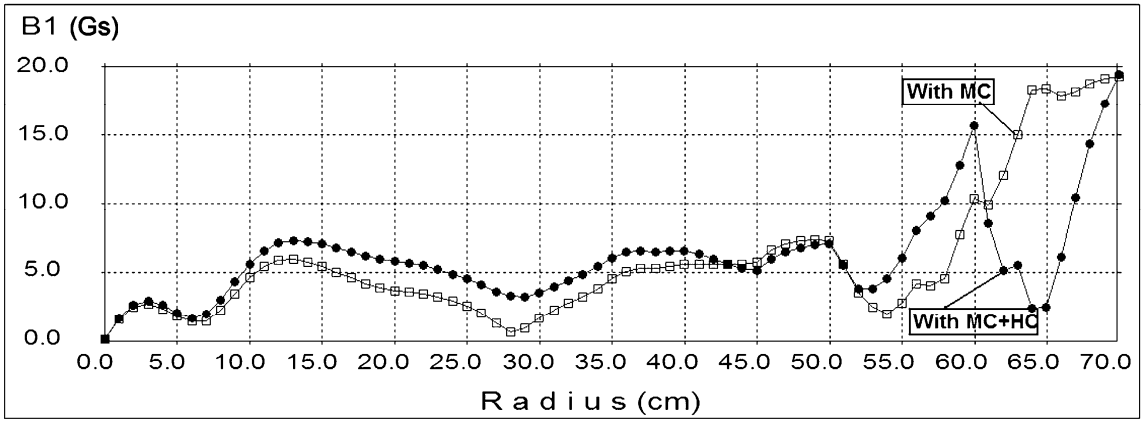

Fig. 2.9. Amplitude of the 1st harmonic with magnetic channels and harmonic coils responses

3 Beam dynamics simulation and experimental results

A diagram of betatron frequencies for AIC-144 cyclotron together with the lines of resonance is presented in Fig. 3.1. The most important resonance is the nonlinear coupling one $Q_r - 2Q_z = 1$ having average magnetic field as driving term. This resonance occurs at energy of 59.5 MeV and, as a rule, leads to large axial losses of the beam. Another important resonance $2Q_z = 1$ is crossed just after the coupling one. This resonance also increases the axial amplitudes of particles if the radial gradient of the 1st harmonic amplitude is too large.

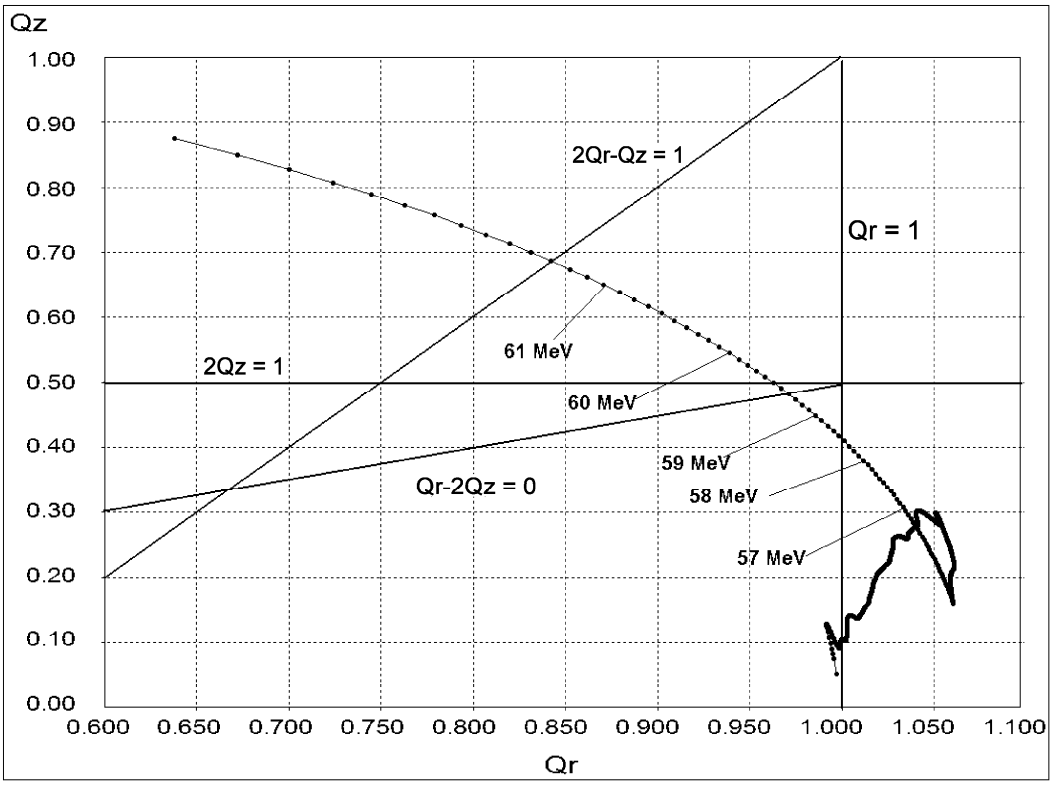

Fig. 3.1. Diagram of betatron frequencies for AIC-144 cyclotron

Almost all calculations of the beam acceleration have been performed starting from an exit slit of ion source (IS) up to the entrance of the 1st deflector. A bunch of 1000 protons with a phase length of 20°RF and transverse emittances $\varepsilon_r = 300\ \pi$ mm x mrad, $\varepsilon_z = 1000\ \pi$ mm x mrad was formed in the IS slit. The initial proton energy was 1 keV. At the beginning of acceleration the protons occupied the phase range (20-40)°RF which corresponded to optimal axial focusing provided by RF field. Position of the IS slit was at a distance of 4.5 mm from the puller entrance. Radius of IS slit was equal to 25 mm.

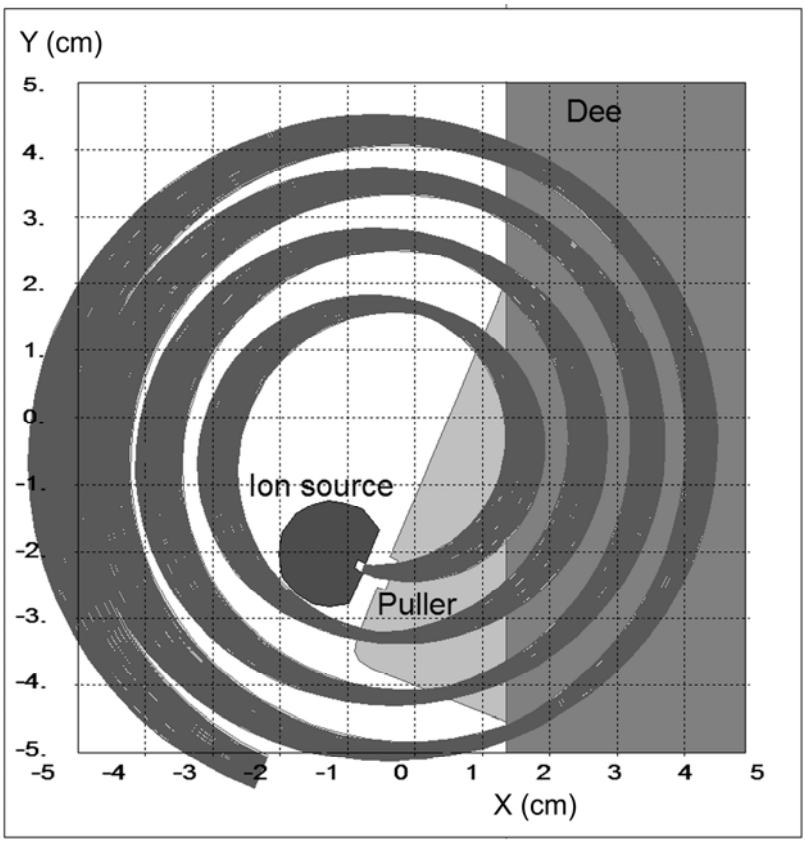

Fig. 3.2. Plan view of the cyclotron center with trajectories of 1000 protons during first 4 turns

The calculations were done for the maximal magnetic field bump and for the one reduced by 130 Gs (see Fig. 2.3). In order not to overload the paper, the results below refer only to the reduced bump that corresponds to maximum of the achieved extraction efficiency. Plan view of the protons trajectories within the first 4 turns is shown in Fig. 3.2.

Different view of the orbits to the left and to the right of the Fig. 3.2 proves the presence of remarkable coherent radial amplitude of the beam at the first turns. Indeed, as it is shown in Fig. 3.3, the beam is injected with radial coherent shift of about 6 mm, then the amplitude of coherent oscillations increases up to 11 mm at radius 25 cm due to action of the 1st harmonic of the magnetic field. Beyond radius 25 cm the coherent amplitude experiences a beating in the range 6-10 mm. At the end of acceleration (radius 63 cm) due to experimentally chosen distribution of the amplitude and phase of the 1st harmonic the coherent amplitude is quickly decreased to 4 mm. This optimal distribution of the 1st harmonic was provided by two pairs of the special harmonic coils.

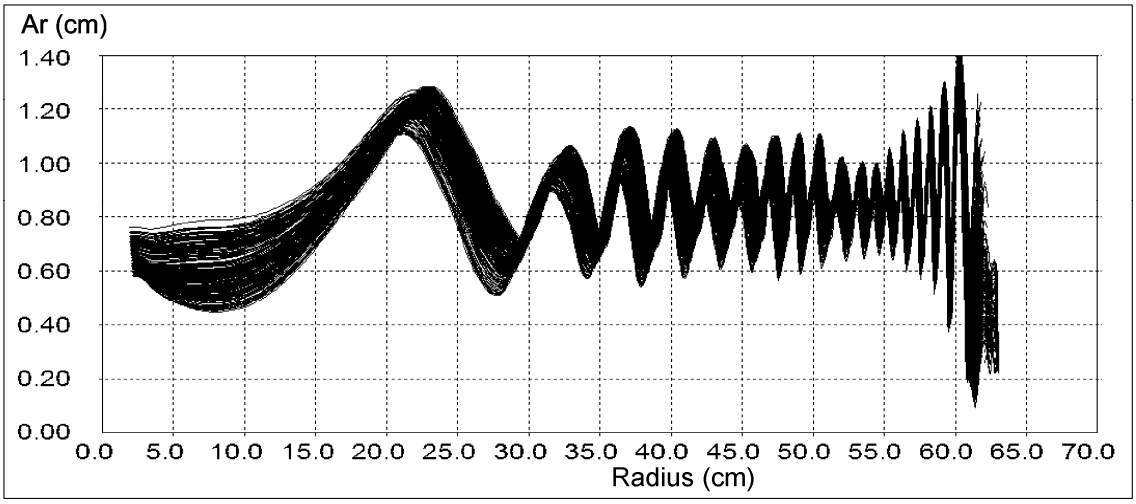

Fig. 3.3. Amplitudes of proton radial oscillations versus average radius of the orbit

Coherent shift at the beam injection occurs due to not optimal radial position of the puller. The puller gap is currently located at radius 25 mm, while its optimal position, arising from the computations, should be 20 mm. Unfortunately, shift of the puller inside is not a trivial task and it is planned to be done in a future. Despite such conditions the achieved beam parameters (when it approaches to extraction system) are good enough to provide extraction efficiency ~50% after three electrostatic deflectors.

Computed axial profile of the beam in full acceleration region is presented in Fig. 3.4. Vertical size of the beam changes in accordance with radial dependence of function $1/Q_z^{\frac{1}{2}}$ in main acceleration region. Only directly before the extraction (radius 60-62 cm) the axial amplitudes of essential part of the protons increase mainly due to the action of nonlinear coupling resonance $Q_r-2Q_z = 0$. Driving term of this resonance is nonlinearity of the average magnetic field which has a large value at the edge of the magnet pole. The value of the driving term cannot be changed and only a good quality of the beam permits to limit axial losses of the beam. Radial amplitudes of the protons should be small enough to restrict axial losses of the protons on a dee. Computations show that if distribution of the radial amplitudes is in the range 2-6 mm (see Fig. 3.3) then the axial losses comprise ~40%. It should be noted that the resonance $2Q_z=1$ gives additional impact on the axial amplitudes grow. Since the resonanses $Q_r-2Q_z = 0$ and $2Q_z = 1$ are located very close to each other, it is difficult to distinguish their actions.

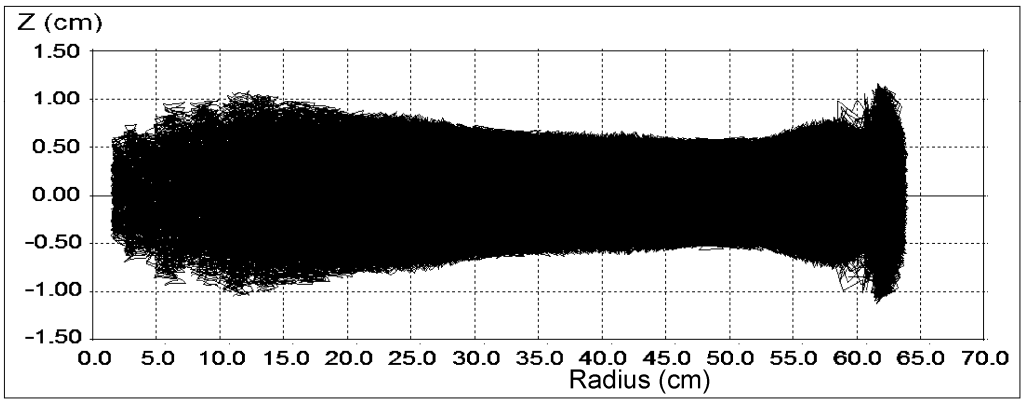

Fig. 3.4. Calculated axial profile of the beam

Phase motion of the beam has been measured with the Smith and Garren method [5, 6]. To implement this procedure, at different radial positions of the integral probe signed N3, a value of the beam current was measured at four main coil currents which were decreased step by step. The first point is working current in the main coil, the 2-nd one corresponds to a moment when the beam current begins to decrease, the 3-rd one is fixed when the beam current is equal half of maximum in the radius described and the 4-th one is taken when the beam becomes equal zero. An example of such series of the Smith and Garren curves is shown in Fig. 3. 5.

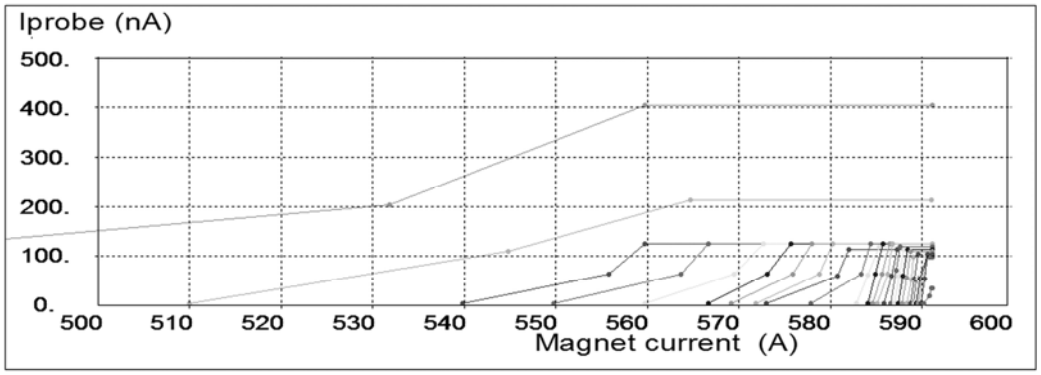

Fig. 3.5. Smith and Garren curves measured for a radial range of probe position 6-62 cm

This simple method after using the appropriate mathematical procedure made it possible to achieve the phase motion of the beam center with quite good accuracy. A comparison of the two phase curves obtained with the help of this method for initial magnetic field with bump in center 360 Gs and for the one decreased by 130 Gs can be observed in Fig. 3.6. Both phase curves have been obtained after experimental optimization of the main coil current aiming at achieving the extraction maximal efficiency. It occurs if the phase of the beam just before the extraction is ~10°RF.

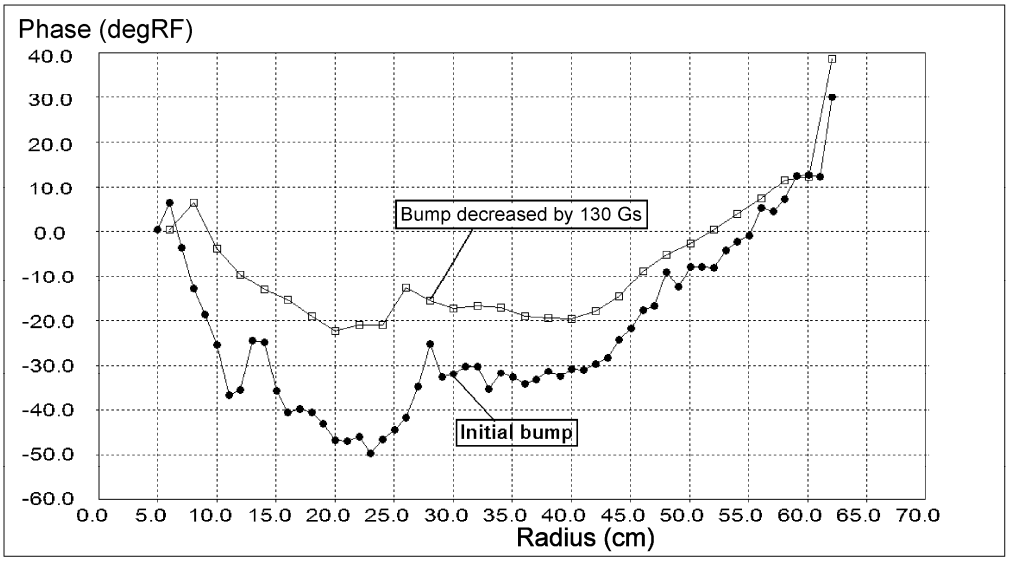

Fig. 3.6. Comparison of the two phase curves obtained for different distributions of the average field shown in Fig. 2.3

Hence, experimental optimization of the beam extraction was finally fulfilled by means of small tuning of the main coil current in every investigated regime. In the beam computation, similar view of the phase motion was obtained using a small tuning of radio frequency since it was difficult to take into account in the simulation a small change of the main current. Computed phase motion of the beam for the bump decreased by 130 Gs is presented in Fig. 3.7. This result was obtained using frequency 26.268 MHz instead of 26.26 MHz which is used in practice.

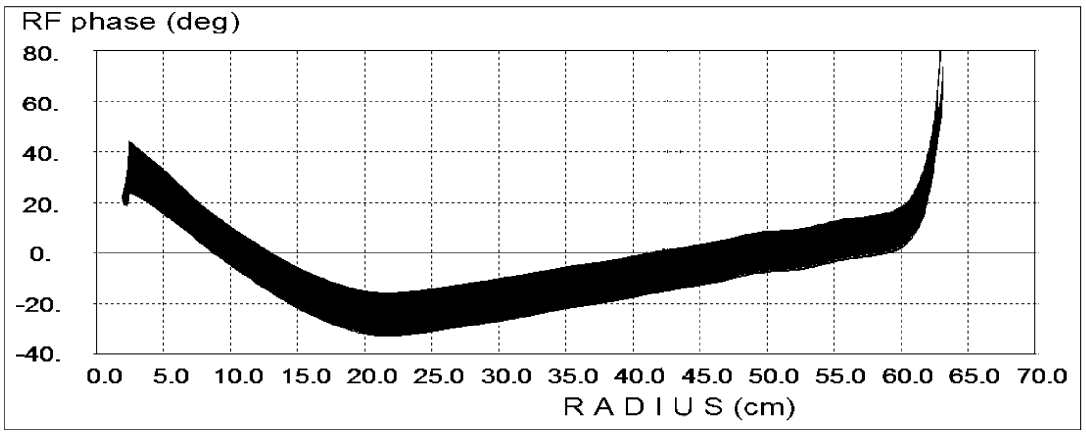

Fig. 3.7. Calculated phase motion of 1000 protons for the decreased bump and f = 26.268 MHz

Calculated positions of protons on the transverse phase planes at entrance of the 1st deflector are shown in Fig. 3.8. Radial position of the 1st deflector septum was changed during optimization procedure. The purpose was to obtain maximal number of protons at the

entrance of the deflector from 1000 ones started in the ion source slit. It was found that radius 628 mm corresponded to this requirement. Approximately 50% of protons appeared at deflector entrance. The others were lost vertically on the dee (~38%) and at the front face of the septum (~12%) of the 1st deflector. Root mean square values of the beam emittances are $\varepsilon_r \approx 6\ \pi$ mm•mrad, $\varepsilon_z \approx 32\ \pi$ mm•mrad. Energy distribution of extracted beam is illustrated in Fig. 3.9. Average energy of the proton beam is 60.7 MeV, energy spread is ±0.5%.

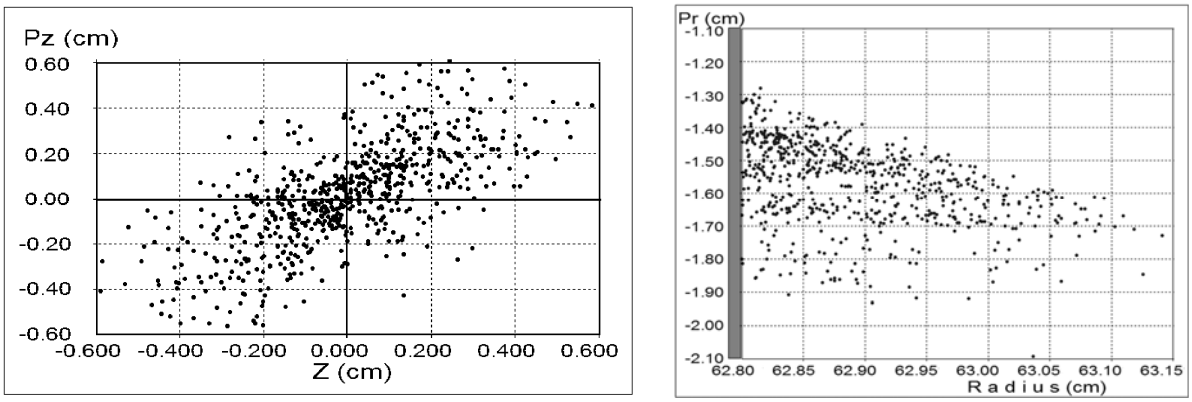

Fig. 3.8. Position of protons on transverse phase planes at entrance of the 1st deflector. Left – axial plane, right – radial plane.

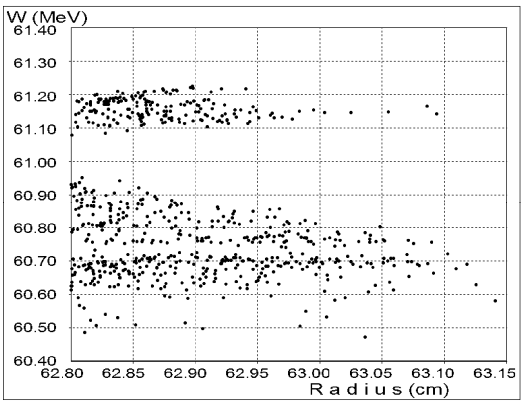

Fig. 3.9. Position of protons on plane radius-energy at entrance of the 1st deflector

Scheme of the first part of extraction system is shown in Fig. 3.10. It consists of three electrostatic deflectors ESD1, ESD2 and ESD3. The last two ones are located in common construction but they have different cross section of the electrodes. ESD2 has flat electrodes while ESD3 has profiled ones in vertical direction in order to provide additional focusing of the beam in the horizontal plane. ESD1 has flat electrodes.

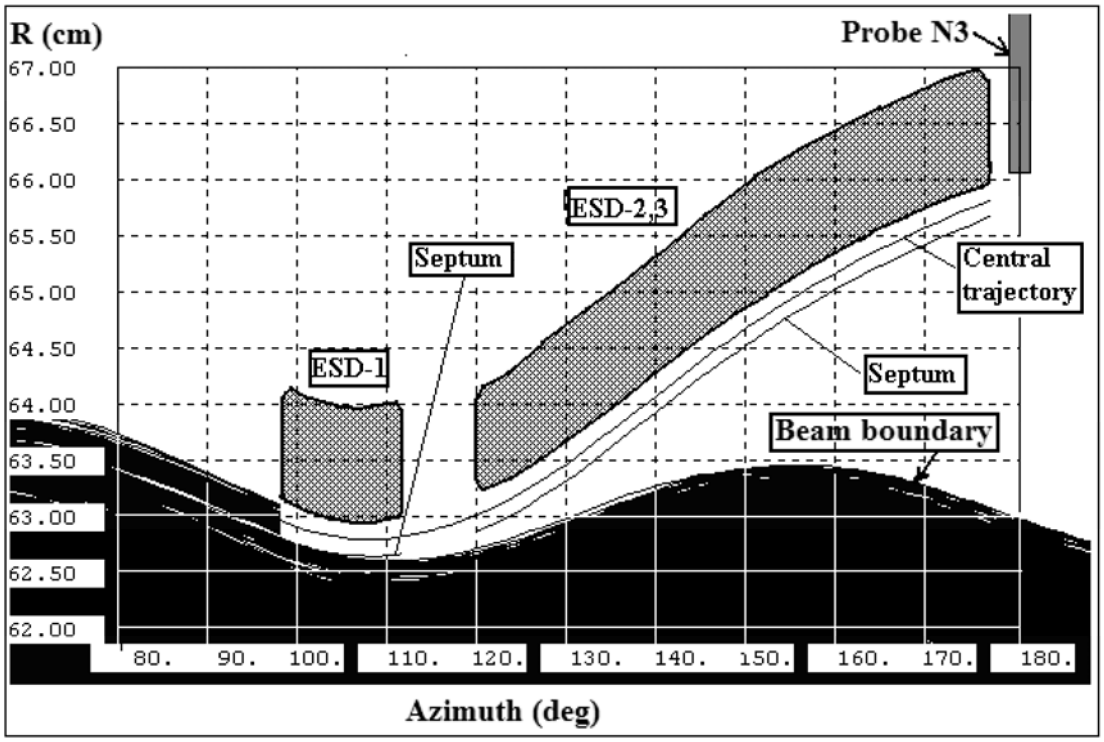

Fig. 3.10. Scheme of the first part of extraction system

The best extraction efficiency has been experimentally achieved after the following sequence of tuning parameters:

- bump of magnetic field in the center of cyclotron;
- distance between ion source and puller;
- position of all elements of extraction system;
- currents in harmonic coils.

Main beam current probe N3 has been used in those optimization procedures to measure radial distribution of the beam intensity through full acceleration region and through extraction one as well. It has current lamella $\Delta r \times \Delta z \times (r \times \Delta\varphi) = 20\text{x}18\text{x}20$ mm^3 (φ – is azimuth direction). Since the probe is located just after the ESD3 exit, it can be used for direct estimation of the extraction efficiency after the first part of extraction system. Figure 3.11 shows beam current measured by probe N3 beginning from radius 6 cm and Fig. 3.12 presents these data in enlarged scale beginning from 50 cm. It can be observed that extraction efficiency after deflectors is close to 50%. This value is in very good agreement with the results of beam simulation described above. Overall efficiency has been estimated in point C2 which is located at a distance ~2 m from the cyclotron. Value of this efficiency ~35% is also indicated in Fig. 3.12. Approximately 15% of protons are lost in three magnetic channels.

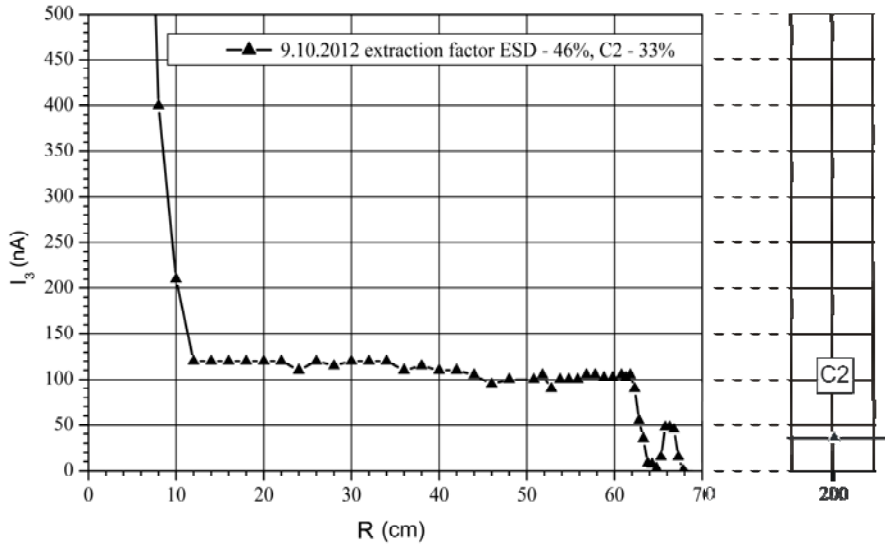

Fig. 3.11. Beam current measured by probe N3 in the full radial range

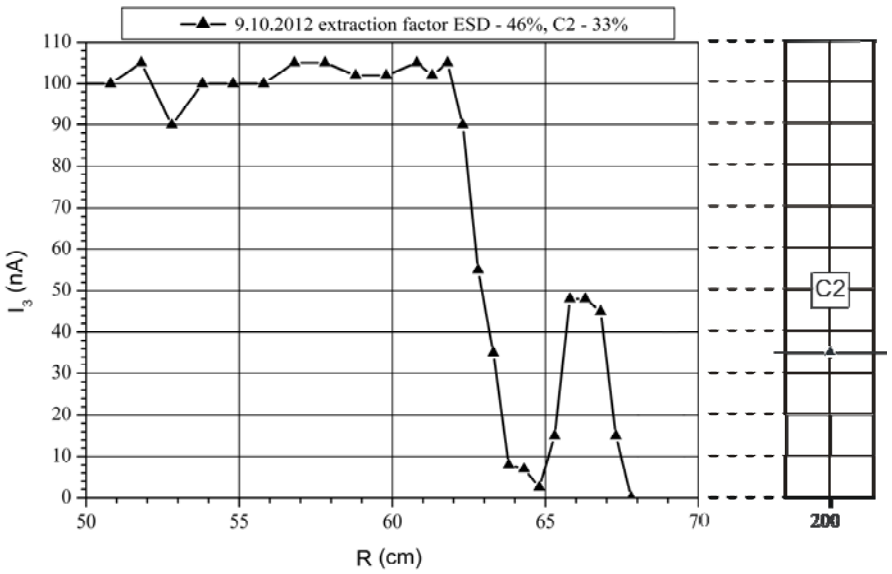

Fig. 3.12. Beam current measured by probe N3 from radius 50 cm. Current in point C2 is also indicated.

Conclusions

Proton beam in AIC-144 cyclotron is accelerated without large losses in radial region 12-62 cm and is extracted from the cyclotron with pretty good overall efficiency ~35%.

The beam has been used for the first time for successful treatment of 11 patients in 2011 and 4 patients in 2012. The cyclotron is now ready to deliver 60 MeV proton beam for a long-term radiotherapy of 50 patients with eye melanoma in the year 2013 .

References

1. B. Romanowska-Dixon i in. Polskie badania i wdrożenia w onkologii-radioterapia protonowa w nowotworach oka. Konferencja Onkologia 2011. Warszawa 18.10.2011

2. K. Daniel i in. Symetryzacja pola magnetycznego cyklotronu AIC-144. Raport 2052/AP, IFJ PANS, Krakow, 2011.

3. I. V. Amirkhanov, G.A. Karamysheva, I.N. Kiyan, J. Sulikowski. Mathematical Simulation of the Main Operation Mode of the AIC-144 Multipurpose Isochronous Cyclotron. // ISSN 1547-4771, Physics of Particles and Nuclei Letters, 2012, Vol. 9, No. 4–5, pp. 394–397.

4. A. A.Garren and Lloyd Smith, Diagnosis and Correction of Beam Behavior in Isochronous Cyclotron, Proc. of the Int. Conference on Sector-Focused Cyclotrons and Meson Factories, Geneva, 1963.

5. Herve Marie, How to Use Smith and Garren Curves to Correct Isochronism, IBA internal report, 1993.

6. K. Daniel i in. Przystosowanie cyklotronu AIC-144 do protonowej terapii oka. Maksymalizacja energii protonów, rewitalizacja generatora w,cz. Raport 2006/AP, IFJ PAN, 2007.